

2nd International Conference on Structural Integrity, ICSI 2017, 4-7 September 2017, Funchal, Madeira, Portugal

# A comparative study between conventional and elevated temperature creep autofrettage

Volodymyr Okorokov\*, Yevgen Gorash

*University of Strathclyde, Technology & Innovation Centre, 99 George Street, Glasgow G1 1RD, Scotland, UK*

---

## Abstract

This paper presents a comparative study between conventional hydraulic and elevated temperature autofrettage. For modelling of both methods advanced plasticity and creep material models are used. The main governing equations for the models are presented as well. A beneficial influence of compressive residual stresses induced by both methods is demonstrated on a benchmark problem of cross bored block. The effectiveness and applicability of the two methods are estimated by conduction of compressive residual stress analysis and crack arrest modeling. Numerical simulation of the cyclic plasticity and creep problems are carried out by means of FEM in ANSYS Workbench with FORTRAN user-programmable subroutines for material model incorporating custom equations.

© 2017 The Authors. Published by Elsevier B.V.

Peer-review under responsibility of the Scientific Committee of ICSI 2017

## Keywords:

Crack arrest, Creep autofrettage, Finite Element Analysis, Plasticity, Compressive residual stress

---

## 1. Introduction

Application of the autofrettage processes has become a useful tool of increasing the fatigue resistance for many high pressure components working in dynamic conditions. Nowadays, several types of autofrettage such as hydraulic, swage, thermal autofrettage and combination of autofrettage with shrink fitting technology are extensively used in different industries. This paper is mainly concentrated on the effect of hydraulic autofrettage which is applicable for a huge variety of high pressure parts with highly stressed locations due to sharp corners of bore intersections. The main idea of hydraulic autofrettage is to apply high pressure to the internal surface of a high pressure component in order to induce a plastic strain of required values. With unloading the elastic layers of a component start shrinking the plastically deformed layers thereby inducing compressive stresses. There have been numerous studies regarding to hydraulic autofrettage modelling starting from a simple analytical close solution (Adibi-Asl and Livieri, 2006; Wahi et al., 2011; Trojnecki and Krasiński, 2014) and ending with quite comprehensive models which include accu-

---

\* Corresponding author. Tel.: +44-787-4275442 ; fax: +44-141-5520775.

E-mail address: [volodymyr.okorokov@strath.ac.uk](mailto:volodymyr.okorokov@strath.ac.uk)

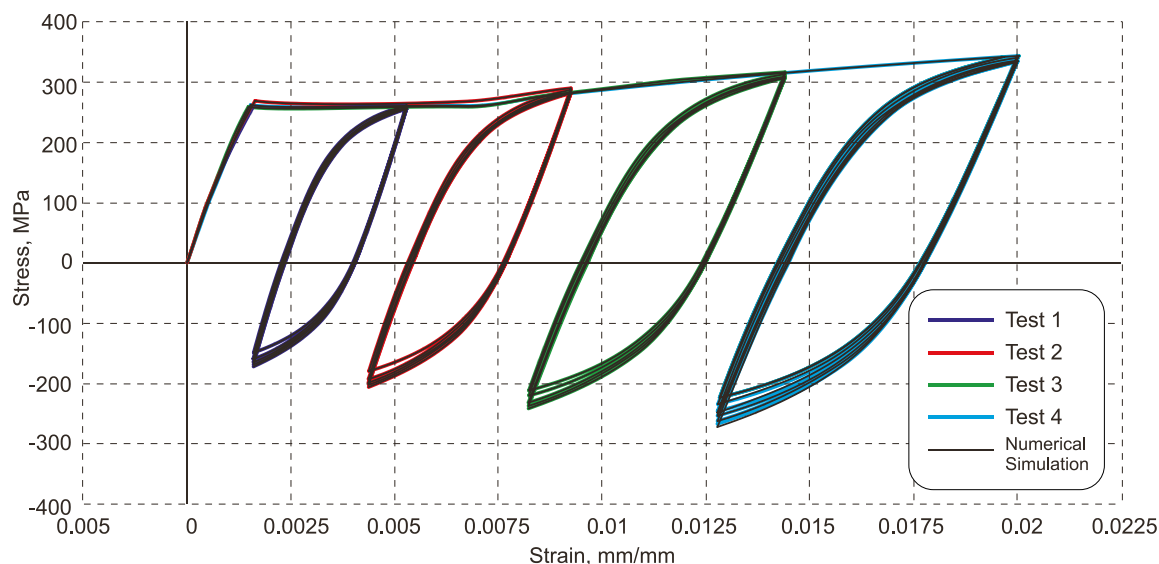


Fig. 1. Cyclic plasticity material response.

rate material behavior and fatigue lifetime prediction (Jahed et al., 2006; Parker and Underwood, 1999). Nevertheless, such research questions as the accurate material behavior modelling and fatigue lifetime prediction of autofrettaged components with high stress concentration locations are still open.

Conventional hydraulic autofrettage assumes application of overload pressure at ambient temperature. However, studies by Berman and Pai (1967, 1969) showed that application of autofrettage pressure at elevated temperature can provide some benefits over conventional ambient temperature autofrettage. Overload pressure in the case of elevated temperature autofrettage is significantly lower than that pressure for hydraulic autofrettage as inelastic creep strains are induced at a smaller level of stresses. This may be more favorable for the cases where the application of very high pressure in autofrettage assemblies may cause structural damage. That type of autofrettage can also provide a deeper level of compressive residual stresses compared to conventional autofrettage. In spite of the potential benefits of creep autofrettage, this problem has not got much attention since the first publications. This may be explained by a lack of the knowledge of the material properties under conditions of creep deformation and modelling techniques which are able to simulate creep compressive residual stresses. One of the objectives of this study is, therefore, to extend conventional hydraulic autofrettage to an elevated temperature autofrettage application with inducing creep strains.

Another problem for the autofrettage processes in general is prediction of the fatigue lifetime under the influence of compressive residual stresses. Despite the fact that compressive residual stresses can significantly improve the fatigue lifetime of high pressure components the mechanism of fatigue failure under the influence of compressive residual stresses is not always clear. The dominant part of the fatigue lifetime in components without compressive residual stresses is the crack initiation stage and as soon as a crack is initiated at the surface it immediately propagates inside a component causing fatigue failure. Time for the crack propagation in this case varies from tens to hundreds of cycles which is significantly less than crack initiation time. However, this may not be the case of components with high compressive residual stresses where an initiated crack can be arrested at some point of the propagation.

Herz et al. (2011) show that the prediction of the fatigue failure should depend on the mechanism of failure associated with the presence of compressive residual stresses. For the case of component testing without introducing compressive residual stresses the calculation of crack initiation lives according to local strain based approach had a close prediction to the experimental results. Calculation of the crack propagation life in this case showed negligible effect compared to the initiation life. The situation is different for the case of testing samples with induced compressive residual stresses. A better prediction of fatigue failure is achieved by the crack growth calculation and it is clearly demonstrated that the fatigue endurance limit is related to the crack arrest phenomenon. The crack arrest phenomenon is also more likely to happen in the case of high pressure components working in aggressive corrosion environments, where cracks are initiated at significantly lower levels of stress compared to non-corrosive environments.

If the crack arrest phenomenon is dominant in the fatigue life of autofrettaged part elevated temperature autofrettage can provide higher fatigue life as the compressive residual stress field is deeper compared to the conventional autofrettage case. The compressive residual stress field is also distributed more uniformly over a whole pressure part.

Prediction of the crack arrest is a complex problem as it requires the knowledge not only of fracture material parameters and crack propagation laws but an actual inelastic behavior of a material which is necessary for an accurate prediction of compressive residual stresses after autofrettage as well. In this work a new concept of modelling nonlinear material behavior under cyclic loading is combined with the crack propagation simulation techniques in order to predict the crack arrest phenomena in autofrettaged components.

## 2. Inelastic material modelling

The phenomenon of nonlinear inelastic deformation is in the base of autofrettage methods. Therefore, the knowledge of material nonlinear response under different loading and temperature conditions is of a high importance for accurate compressive residual stress field predictions. Despite the fact that such compressive residual stress induction methods as autofrettage have successfully been used over years the lack of both experimental data and theoretical modeling of the material inelastic response has still been limiting a huge potential of the autofrettage methods. This section presents results of the material testing and modelling concept for both conventional hydraulic autofrettage and elevated temperature creep autofrettage.

### 2.1. Cyclic plasticity testing

Conventional hydraulic autofrettage is usually performed by application of overload autofrettage pressure at ambient temperature conditions. That means, in order to model this autofrettage process properly, the cyclic plasticity material response under ambient temperature should be obtained and simulated. A low carbon steel structural addressed in this study is equivalent to a big international group of weldable, general-purpose, high-strength structural steels, which includes e.g. *Grade 50 (A, B, C, D)* from British Standard BS4360.

In order to investigate the cyclic and monotonic plasticity behavior, monotonic and cyclic tests with different loading programs have been conducted. The samples for mechanical testing have the following geometry parameters: total length – 140 mm; gauge length – 25 mm; grip section width – 20 mm; gauge section width – 12 mm; thickness – 6 mm. The testing has been done with the use of a 250 kN INSTRON servo-hydraulic testing machine under strain control with a total strain rate of  $5 \cdot 10^{-4} \text{ s}^{-1}$  for both monotonic and cyclic loading. The strain has been measured by an extensometer with 10 mm in gauge length.

Figure 1 illustrates the results from the test with non-zero mean strain which induces the mean stress relaxation. This test is of a particular interest for the autofrettage methods as the test can show a realistic material response similar to that from the application of the autofrettage. This means that applying the overload pressure several times may lead to a deeper level of compressive residual stresses. This fact can be used in autofrettage procedures where increasing the autofrettage pressure is applied via a number of steps. It should be noted that a proper modelling of the effect of re-autofrettage is not possible without a plasticity model that can predict cyclic plasticity accurately.

### 2.2. Cyclic plasticity constitutive modelling

This study presents a constitutive model of cyclic plasticity which is based on the von Mises yield criterion. The yield surface is implemented as follows:

$$f = \sqrt{\frac{3}{2} (\mathbf{S} - \mathbf{X}) : (\mathbf{S} - \mathbf{X})} - R - \sigma_0, \quad (1)$$

where  $\mathbf{S}$  – deviatoric stress tensor;  $\mathbf{X}$  – back stress tensor;  $R$  - isotropic hardening variable;  $\sigma_0$  - initial size of the elastic domain.

The phenomena of cyclic softening and hardening suggest that stable hysteresis loops are achieved after a cycling under a fixed strain range. The present experimental observations show a strong dependence between stabilized stress peaks and strain ranges, thereby exhibiting non-Masing behaviour. In order to describe this type of the material

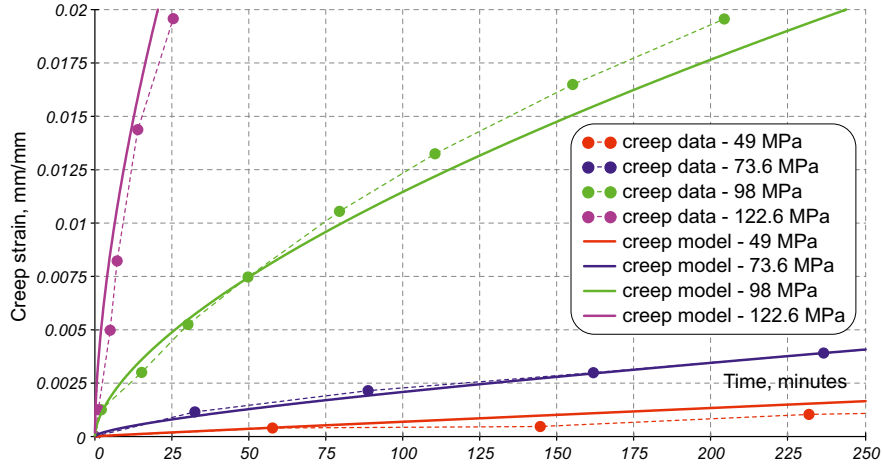


Fig. 2. Creep curves for the structural steel SM50A at 550°C fitted by the “Combined Time Hardening” creep model (7).

behaviour, Chaboche et al. (1979) proposed to use a new internal variable which introduces a dependence of the isotropic hardening asymptotic value on the plastic strain range. The memory surface is introduced as follows

$$F = \sqrt{(\epsilon^p - \zeta)(\epsilon^p - \zeta)} - q, \quad (2)$$

where  $\epsilon^p$  – plastic strain tensor;  $\zeta$  and  $q$  – the centre and the radius of the memory surface, respectively.

Nouailhas et al. (1985) and Ohno (1982) introduced a fading function into the variable  $q$  in order to provide a better agreement with experiments. Despite of the fact that these constitutive models are able to describe a cyclic stress-strain curve quite precisely, there are a few disadvantages of the model. The shape of the monotonic curve as well as the shape of each curve from a cyclic loading is completely determined by a single unified set of equations and parameters calibrated for a cyclic stress-strain curve. That means the monotonic curves for the first cycles will be different from experimental results. To overcome this problem and describe every stress-strain curve for cyclic loading starting from the monotonic curve up to the saturation of stresses, a new set of internal variables is introduced as:

$$\bar{q} = [p - \bar{p} - 2\bar{q}] \delta(Z) \dot{p} \quad \text{and} \quad \bar{p} = [p - \bar{p}] \delta(Z) \dot{p}, \quad (3)$$

where  $\bar{q}$  stand for the rate of strain amplitude that is attained in the previous step and  $\bar{p}$  stand for the rate of accumulated plastic strain that is attained during all straining up to the end of the previous step;  $\delta$  – Dirac delta function the argument of which is defined as follows:

$$Z = \frac{1}{2} [p - p' - \text{sign}(\epsilon_{eq}^p - \bar{\epsilon}_{eq}^p)(\epsilon_{eq}^p - \bar{\epsilon}_{eq}^p)] \quad \text{with} \quad \epsilon_{eq}^p = \sqrt{\frac{2}{3}} \epsilon^p : \epsilon^p. \quad (4)$$

Other components of Eq. (4) are defined as follows

$$\bar{q} = \bar{q}(t - \tau), \quad p' = p(t - \tau), \quad \bar{p} = \bar{p}(t - \tau) \quad \text{and} \quad \epsilon_{eq}^p = \epsilon_{eq}^p(t - \tau), \quad (5)$$

where  $\tau$  is an infinitesimal time delay. The main feature of the above delay differential equations is that the Dirac function returns a required value exactly at the beginning of a new step. At other moments of time the Dirac function returns zero value and the variables remain unchanged during the plastic deformation. This allows the new variables to be constants on the current step of loading and change their value only at the beginning of the next step. The strain range dependence is then introduced into the constants in the isotropic hardening rule and kinematic hardening rule:

$$\dot{R} = b(Q - R)\dot{p} \quad \text{and} \quad \dot{\mathbf{X}}_i = \frac{2}{3}c_i\gamma_i\dot{\epsilon} - \gamma_i\mathbf{X}_i\dot{p}, \quad (6)$$

where  $Q$ ,  $c_i$  and  $\gamma_i$  are functions of the introduced internal variables.

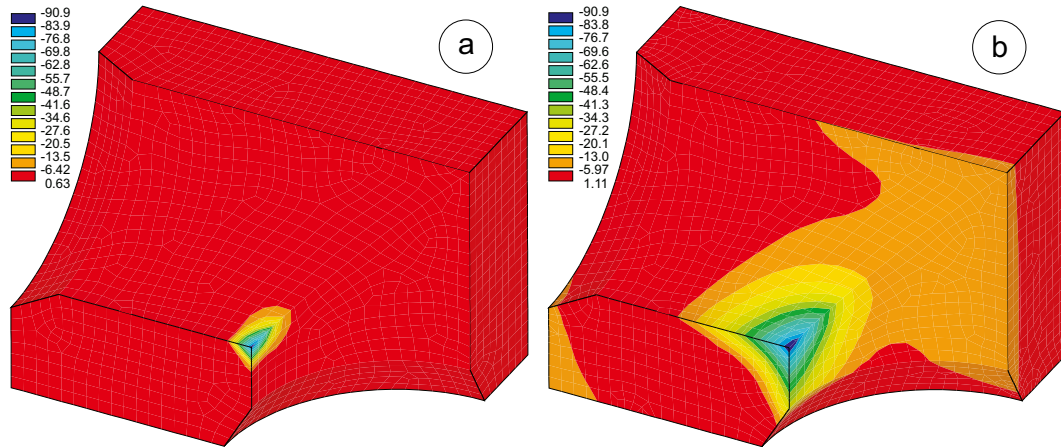


Fig. 3. Compressive residual stress field for conventional autofrettage (a) vs compressive residual stress field for creep autofrettage (b).

### 2.3. Creep data and model

For the purpose of basic feasibility study, the creep constitutive model with constants fitted to available creep test data are all taken from Kodur and Dwaikat (2010). Since performing creep tests at high temperature is very complex and time consuming, at starting stage of research a basic “Combined Time Hardening” creep model is sufficient enough for getting an idea on efficiency of alternative autofrettage approach. This model was selected by Kodur and Dwaikat (2010) from 13 standard creep models available in ANSYS, because it can model both the primary and secondary creep, and is capable of predicting creep strain regardless of any coupling between time and either stress or temperature of steel. The available creep curves at 550°C from Nippon Steel Corporation for the structural steel SM50A, which is close to the steel addressed in this work, were fitted as shown in Fig. 2 by the following equation:

$$\varepsilon^{cr} = \frac{C_1 \sigma^{C_2} t^{C_3+1} e^{-C_4/T}}{C_3 + 1} + C_5 \sigma^{C_6} t e^{-C_7/T}, \quad (7)$$

where the values of creep constants  $C_1 - C_7$  are provided by Kodur and Dwaikat (2010).

### 3. Conventional vs. elevated temperature autofrettage modelling

This section presents an example of the autofrettage simulation for a high pressure component. The high pressure component is presented by a cross-bored steel block specimen proposed by Badr et al. (2000) with material parameters found for a low carbon steel. High pressure parts usually experience cyclic dynamic loading conditions during the service life. Fatigue is, therefore, the main failure mechanism for such high pressure components. Investigation of broken pressure parts with bore intersection shows that the most dangerous location in the part is the sharp corner of the bore intersection. Introduction of the compressive residual stresses by the autofrettage methods into this area can significantly increase fatigue resistance of a high pressure part.

One of the objectives in this study is to show the difference between conventional hydraulic autofrettage and elevated temperature creep autofrettage and define the optimal conditions of applicability for both methods. Conventional hydraulic autofrettage is simulated by applying a high pressure to the internal surface of a high pressure component in order to induce a plastic strain of required values. With unloading the elastic layers of a component start shrinking the plastically deformed layers thereby inducing compressive stresses. The idea of elevated temperature creep autofrettage is similar to the conventional one except for the high temperature that is applied together with autofrettage pressure. The numerical simulation is implemented by means of FEM with the use of ANSYS Workbench. The proposed plasticity and creep models are incorporated into ANSYS Workbench by the means of User Programmable Features (UPF), where user implements custom equations and solving algorithms.

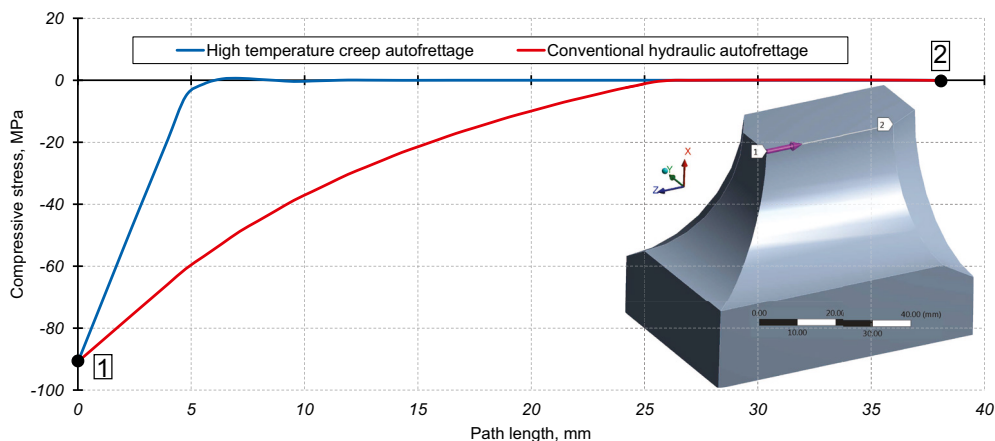


Fig. 4. Comparison of compressive residual stresses along the bore.

Figure 3 demonstrates the result of the autofrettage simulation by both methods. It has been found that in order to induce the magnitude of compressive residual stress of  $-90.9$  MPa in the corner of the bore intersection the pressure of  $27.9$  MPa is required. At the same time only  $11.5$  MPa of pressure is enough to induce the same magnitude of compressive residual stress by elevated temperature creep autofrettage. The distribution of the compressive residual stresses over the distance from the corner is also more favourable in the case of creep autofrettage. It is seen from the Fig. 4 that the compressive residual stresses induced by conventional hydraulic autofrettage quickly disappear just after a few millimetres away from the bore intersection corner. In the case of elevated temperature creep autofrettage the compressive residual stresses are distributed more uniformly over the whole bores. This shows significant benefit of creep autofrettage over conventional autofrettage as this distribution of the compressive residual stresses can provide fatigue crack resistance not only in the corner of the bore intersection but over other locations as well.

However, it should be noted that elevated temperature autofrettage has advantages only within a certain lower pressure range. It is obvious that increasing the autofrettage pressure in conventional autofrettage can give much higher magnitude of the compressive residual stresses. Nevertheless, in the low pressure range creep autofrettage provides compressive residual stresses that cannot be attained by conventional autofrettage at all. As it was pointed out before elevated temperature creep autofrettage can be efficiently applied to high pressure parts where application of extremely high pressure required by conventional autofrettage is not attainable or may cause structural damage to the assembly.

#### 4. Modelling of the crack arrest phenomenon

Once the compressive residual stresses are determined in a pressure part the fatigue life of the part should be predicted. Current fatigue assessment methodology is mainly based on stress and strain based approaches. These methods are usually used for components with blunt features. High stress concentration features like the bore intersections in high pressure pumps can make these methods highly conservative thereby leading to a huge overuse of material. Recently developed theory of critical distance by Taylor (2007) can include high stress gradient into consideration making predictions correlated with experiments. The main idea of this method is to compare stresses obtained from uniaxial tests with stresses averaged over some distance from stress concentration feature instead of applying those uniaxial test data results directly to the point of stress concentration. This method can give good predictions of the fatigue limit by calculating a stress level at which cracks start developing from the component surface. In most of components working without inducing of compressive residual stresses an initiated crack propagates inside a component very fast. This time is negligible compared to time of crack initiation itself. However, if compressive residual stress is present inside a component, an initiated crack can be arrested with propagation. This fact allows applying additional load to a component, so that the fatigue limit is determined by the load required for crack initiation and an additional load required for a crack to propagate before the arrest.

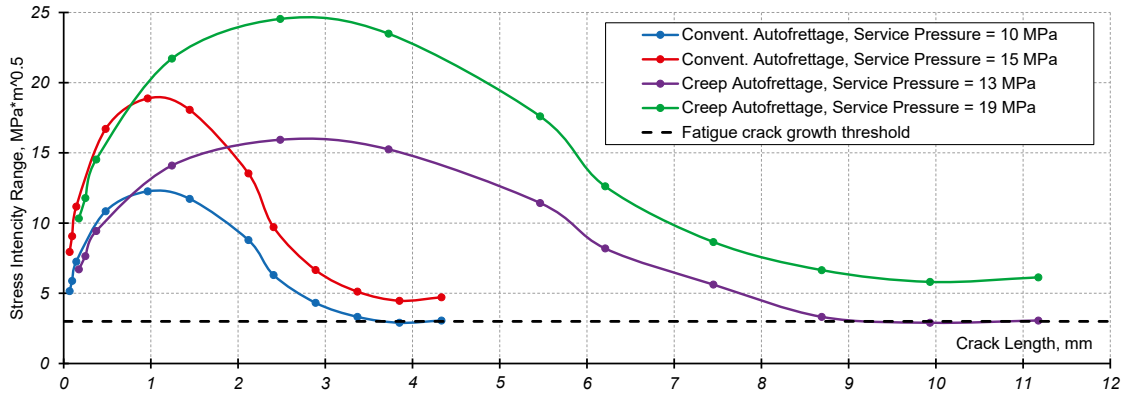


Fig. 5. Stress intensity calculations for conventional and creep autofrettage.

In order to calculate the total load required for crack initiation and propagation application of fracture mechanics approaches is required. In this study the concept of crack closure is used. According to this the effective stress intensity factor range is defined as:

$$\Delta K_{eff} = K_{max} - K_{op}, \quad (8)$$

where  $K_{max}$  – stress intensity factor calculated at maximum load;  $K_{op}$  – stress intensity factor calculated when a crack starts to open; and a crack propagates when the following condition is fulfilled:

$$\Delta K_{eff} > \Delta K_{tr} \quad (9)$$

where  $\Delta K_{tr}$  – effective fatigue crack propagation threshold. For low carbon steels this value can be estimated as 3 [MPa  $\sqrt{m}$ ]. That condition essentially means that if the effective stress intensity factor range is less than the effective crack propagation threshold a crack does not propagate.

One of the objectives in this study is to compare crack arrest analysis for conventional hydraulic autofrettage and for elevated temperature creep autofrettage. As the stress analysis for creep autofrettage has shown a deeper level of compressive residual stresses for the same magnitude of compressive residual stress at the corner of intersected bores a crack initiated at the corner is expected to be arrested at longer length in the case of creep autofrettage compared to conventional autofrettage. In order to conduct the crack arrest analysis an elliptical crack is introduced into the pressure part in the corner of the bore intersection with faces perpendicular to the maximum principal stress direction. Propagation of the crack is simulated by nodal release method (Anderson, 2005).

The main steps of the crack arrest analysis is defined as follows:

1. Defining initial crack length.
2. Applying service pressure to the pressure part. At this stage  $K_{max}$  and  $K_{op}$  are determined using weight function method (Anderson, 2005).
3. If the condition (9) is fulfilled the crack propagates and a new crack front is defined. If the condition (9) is not fulfilled the crack is arrested. The pressure value from the step 2 is then defined as the fatigue limit.
4. Unloading and releasing nodes of crack faces according to the new crack front and repeating the steps 2 and 3.

Figure 5 demonstrates the results of the crack arrest analysis for the pressure part autofrettaged by using both conventional and elevated temperature creep autofrettage. Both methods show similar results with regards to the arrested crack. The crack is allowed to start propagating from the bore intersection. However, with propagating inside the field of high compressive residual stresses the effective crack intensity factor ranges slow down reaching the value of effective fatigue crack propagation threshold. That means the crack is arrested and can only be forced to propagate by increasing the service pressure. The difference between the two methods is that with the use of creep autofrettage the crack is arrested for a longer length and under a higher pressure. Therefore, the pressure part has a higher fatigue limit when elevated temperature autofrettage is used.



## 5. Conclusions

This paper presents the comparative study between conventional hydraulic autofrettage and elevated temperature creep autofrettage. Advanced plasticity and creep material modelling is used for simulation of both autofrettage methods. In order to analyze the effectiveness of the two autofrettage methods the compressive residual stress analysis together with crack arrest analysis are conducted.

Elevated temperature creep autofrettage has advantages over conventional hydraulic autofrettage in the low pressure autofrettage range. This is explained by the fact that the material does not have yield stress during creep deformation, so that creep strains are developed at any level of stress. The results show that creep autofrettage can induce a high magnitude of compressive residual stresses by applying pressure of values similar to working conditions. At this pressure range conventional autofrettage is not applicable at all. This makes creep autofrettage very attractive for the applications where high autofrettage pressure can cause structural damage.

Conventional autofrettage shows a very high compressive residual stress magnitude in the bore intersection location of a high pressure part. However, these stresses decrease rapidly moving away from the stress concentration. Elevated temperature creep autofrettage can provide a deeper level of compressive residual stresses with a high magnitude of these stresses even far away from the stress concentration. This allows a longer crack to be arrested in the pressure part under a higher service pressure compared to conventional autofrettage. Potentially, the biggest benefit of the two autofrettage methods can be attained by its combination. In this case a very high magnitude of compressive residual stresses can be induced in the bore intersection by conventional autofrettage. Whereas elevated temperature creep autofrettage can provide a high level of compressive residual stresses away from the stress concentration.

## Acknowledgements

This study was implemented in the frames of H2020 European Industrial Doctorate project (ref. 643159) titled “Advanced Pump Engineering for Severe Applications” (APESA – [www.apesaproject.eu](http://www.apesaproject.eu)) initiated by the University of Strathclyde and Weir Minerals.

## References

- Adibi-Asl, R., Livieri, P., 2006. Analytical approach in autofrettaged spherical pressure vessels considering the bauschinger effect. *J. of Pressure Vessel Technology* 129(3), 411–419.
- Anderson, T.L., 2005. *Fracture Mechanics: Fundamentals and Applications*. 3rd ed., CRC Press, Boca Raton, FL.
- Badr, E., Sorem, J., Tipton, S., 2000. Evaluation of the autofrettage effect on fatigue lives of steel blocks with crossbores using a statistical and a strain-based method. *J. of Testing and Evaluation* 28(3), 181–188.
- Berman, I., Pai, D.H., 1967. Elevated temperature autofrettage. *J. of Engineering for Power* 89(3), 369–375.
- Berman, I., Pai, D.H., 1969. Creep autofrettage. U.S. Patent 3,438,114. URL: <http://www.google.co.uk/patents/US3438114>.
- Chaboche, J.-L., Dang Van, K., Cordier, G., 1979. Modelization of the strain memory effect on the cyclic hardening of 316 stainless steel, in: *Trans. 5th Int. Conf. on Structural Mechanics in Reactor Technology. IASMiRT, Berlin, Germany. number L11/3 in SMiRT5*, pp. 1–10.
- Herz, E., Hertel, O., Vormwald, M., 2011. Numerical simulation of plasticity induced fatigue crack opening and closure for autofrettaged intersecting holes. *Engineering Fracture Mechanics* 78(3), 559–572.
- Jahed, H., Farshi, B., Hosseini, M., 2006. Fatigue life prediction of autofrettage tubes using actual material behaviour. *Int. J. of Pressure Vessels & Piping* 83(10), 749–755.
- Kodur, V.K.R., Dwaikat, M.M.S., 2010. Effect of high temperature creep on the fire response of restrained steel beams. *Materials & Structures* 43(10), 1327–1341.
- Nouailhas, D., Cailletaud, G., Policella, H., Marquis, D., Dufailly, J., Lieurade, H., Ribes, A., Bollinger, E., 1985. On the description of cyclic hardening and initial cold working. *Engineering Fracture Mechanics* 21(4), 887–895.
- Ohno, N., 1982. A constitutive model of cyclic plasticity with a nonhardening strain region. *J. of Applied Mechanics* 49(4), 721–727.
- Parker, A.P., Underwood, J.H., 1999. Influence of bauschinger effect on residual stress and fatigue lifetimes in autofrettaged thick-walled cylinders, in: *Panontin, T.L., Sheppard, S.D. (Eds.), Fatigue and Fracture Mechanics: vol. 29, ASTM STP 1332. American Society for Testing and Materials, West Conshohocken, PA, USA*, pp. 565–583.
- Taylor, D., 2007. *The Theory of Critical Distances: A New Perspective in Fracture Mechanics*. Elsevier Science Ltd, Oxford.
- Trojnacki, A., Krasinski, M., 2014. Numerical verification of analytical solution for autofrettaged high-pressure vessels. *J. of Theoretical & Applied Mechanics* 52(3), 731–744.
- Wahi, N., Ayob, A., Kabashi Elbasheer, M., 2011. Effect of optimum autofrettage on pressure limits of thick-walled cylinder. *Int. J. of Environmental Science & Development* 2(4), 329–333.